applied sciences

MDPI

Article

A Numerical Bio-Geotechnical Model of Pressure-Responsive Microbially Induced Calcium Carbonate Precipitation

Jianye Wang [1], Helen Mitrani [2], Anil Wipat [3], Polly Moreland [3], Jamie Haystead [4], Meng Zhang [4] and Martyn Dade Robertson [5,*]

[1] School of Civil Engineering and Transportation, Beijing University of Civil Engineering and Architecture, Beijing 100044, China; wangjianye@bucea.edu.cn
[2] Civil Engineering, School of Engineering, Newcastle University, Newcastle upon Tyne NE1 7RU, UK
[3] School of Computing, Newcastle University, Newcastle upon Tyne NE1 7RU, UK
[4] Hub for Biotechnology in the Built Environment, Department of Applied Sciences, Northumbria University, Newcastle upon Tyne NE1 7RU, UK
[5] Hub for Biotechnology in the Built Environment, Department of Architecture and Built Environment, Northumbria University, Newcastle upon Tyne NE1 7RU, UK
* Correspondence: martyn.dade-robertson@northumbria.ac.uk

Abstract: The employment of Microbially Induced Calcium Carbonate Precipitation (MICP) is of increasing interest as a technique for environmentally sustainable soil stabilisation. Recent advancements in synthetic biology have allowed for the conception of a pressure-responsive MICP process, wherein bacteria are engineered to sense environmental loads, thereby offering the potential to stabilise specific soil regions selectively. In this study, a 2D smart bio-geotechnical model is proposed based on a pressure-responsive MICP system. Experimentally obtained pressure-responsive genes and hypothetical genes with different pressure responses were applied in the model and two soil profiles were evaluated. The resulting model bridges scales from gene expression within bacteria cells to geotechnical simulations. The results show that both strata and gene expression–pressure relationships have a significant influence on the distribution pattern of calcium carbonate precipitation within the soil matrix. Among the evaluated experimental genes, Gene A demonstrates the best performance in both of the two soil profiles due to the effective stabilisation in the centre area beneath the load, while Genes B and C are more effective in reinforcing peripheral regions. Furthermore, when the hypothetical genes are utilised, there is an increasing stabilisation area with a decreased threshold value. The results show that the technique can be used for soil reinforcement in specific areas.

Keywords: microbially induced calcium carbonate precipitation (MICP); responsive materials; synthetic biology; bio-mediated soil stabilisation

Citation: Wang, J.; Mitrani, H.; Wipat, A.; Moreland, P.; Haystead, J.; Zhang, M.; Robertson, M.D. A Numerical Bio-Geotechnical Model of Pressure-Responsive Microbially Induced Calcium Carbonate Precipitation. *Appl. Sci.* **2024**, *14*, 2854. https://doi.org/10.3390/app14072854

Academic Editor: Tiago Miranda

Received: 6 February 2024
Revised: 5 March 2024
Accepted: 26 March 2024
Published: 28 March 2024

1. Introduction

To address the construction challenges posed by weak or problematic soils, the implementation of ground improvement methods becomes imperative, aiming to augment the soil's strength and stiffness. Conventional soil improvement techniques, such as chemical grouting or mixing methods [1–3], have not only resulted in a high carbon footprint but can also lead to environmental problems and ecosystem disturbance [4,5]. Consequently, Microbially Induced Calcium Carbonate Precipitation (MICP) is emerging as an innovative and sustainable ground improvement method, characterised by its lesser pollution and relatively cost-effective nature [6,7]. This technique improves soil properties by filling void spaces and forming bonds at interparticle contacts with calcium carbonate precipitation catalysed by ureolytic bacteria. Numerous laboratory investigations have demonstrated the efficacy of MICP in enhancing soil strength, stiffness, and reducing permeability [8–16]. Furthermore, field applications have validated its practical feasibility [17–19]. To optimise the MICP process further, numerical models have also been produced, which include

aspects such as reaction rates, fluid flow, bacteria cell concentrations, and the resulting concentration of calcium carbonate, alongside the reduction in soil permeability [20–24].

Despite the evident advantages of MICP, the difficulty in using it as a ground improvement method is in achieving uniform $CaCO_3$ formation and associated mechanical strength [25,26]. Some investigations have proposed innovative grouting methods to address this issue [27,28]; however, these solutions have been primarily evaluated at the laboratory scale. An alternative approach to solve this problem is to use synthetic biology [29] to engineer a biological system capable of controlled precipitation as needed. Recent advancements in the realm of synthetic biology, as reported by [30], have spurred the hypothesis that it could pave the way for the creation of a system wherein soil could be inoculated with genetically engineered bacteria. These bacteria, in response to increased pressure, could catalyse the formation of calcium carbonate crystals, binding soil particles and thereby enhancing soil strength in areas subjected to external loads. Such a system holds the potential to transform soils into a significant smart Engineered Living Material (ELM) type. The system is based on the idea that bacteria can detect and react to alterations in water pressure as the soil is loaded. These changes can act as input stimuli to a gene circuit which triggers the genetic element responsible for inducing calcium carbonate. Previously, prospective mechanisms for genetic responses to heightened pressure have been identified in two 'model' organisms, namely Escherichia coli [31] and Bacillus subtilis. The latter, a common soil-dwelling bacterium, although displaying limited natural Microbially Induced Calcium Carbonate Precipitation (MICP) capabilities, holds promise as a potential chassis organism, serving as a platform for engineering an MICP process. In the experiments, it has also been shown that there is no straightforward genetic response to elevated load. Instead, different genetic sensitivities to environmental stresses have been observed.

In this study, by engineering the bacteria with pressure-sensing capabilities, it is anticipated that they can be tuned to respond to various pressures and environmental conditions. This tuning could enable the programmed production of diverse distributions of calcium carbonate precipitation. Designing such a smart system requires the development of a computational model which can bridge the gap between geotechnical models describing load and water pressures through the soil and the genetic responses of our selected bacterium and help design new hypothetical engineered material responses. This computational model serves as an indispensable tool in designing hypothetical engineered material responses, thus laying the foundation for pioneering advancements in the field.

2. Background

2.1. MICP through Ureolytic Hydrolysis

MICP mediated by bacterial urease is well studied in the literature. Several different reactions occur during this process. These include ureolysis (Equation (1)), the protonation of NH_3 (Equation (2)), CO_2 hydrolysis (Equation (3)), the dissociation of carbonic acid (Equation (4)), the dissociation of bicarbonate (Equation (5)) and $CaCO_3$ precipitation/dissolution (Equation (6)).

$$CO(NH_2)_2 + H_2O \rightarrow 2NH_3 + CO_2 \quad (1)$$

$$2NH_3 + 2H_2O \longleftrightarrow 2NH_4^+ + 2OH^- \quad (2)$$

$$CO_2 + H_2O \longleftrightarrow H_2CO_3 \quad (3)$$

$$H_2CO_3 + OH^- \longleftrightarrow HCO_3^- + H_2O \quad (4)$$

$$HCO_3^- + OH^- \longleftrightarrow CO_3^{2-} + H_2O \quad (5)$$

$$CO_3^{2-} + Ca^{2+} \rightarrow CaCO_3\downarrow \quad (6)$$

Many factors control and guide the ureolytic MICP process. These include the type of microbe (in terms of urease activity produced and extracellular polymeric substances (EPS) components), calcium ion concentrations, urea concentration, other chemical elements

within the surroundings (for example Mg^{2+}), cell number in terms of nucleation sites, temperature, etc.

2.2. Synthetic Biology

Synthetic biology is a discipline associated with the 'rational' engineering of biological systems through an approach that combines genetic engineering with computational modelling and engineering principles for the design of new biological systems. Synthetic biology is related to fields including computational software and hardware, electrical and civil engineering in describing biological systems as hierarchies of parts with integrated inputs and outputs [32]. A core concept in synthetic biology is the central dogma. Genes within living cells are transcribed into mRNA, which is subsequently translated into amino acid sequences which assemble to form proteins [33]. These proteins perform the structural and functional work of the cell. Both transcription and translation are regulated. In transcriptional regulation, this means that the level of production of a particular gene can be controlled through a genetic element, which is often described as a promotor. These promotors act like switches and can be sensitive to a range of physical and chemical signals. The genes following a specific promoter can be swapped to engineer a cell that has programmed output in response to a specific signal. However, biological systems are not as easy to engineer as mechanical or electrical systems and synthetic biology also involves a design cycle that includes computational modelling, testing and refinement to minimise the need for experiments. In this paper, we present a novel computational model which allows us to map between gene responses derived from real biological data and soil. The model acts as both a simulation and a computer-aided design tool, allowing us to identify optimal genetic responses for specific conditions.

2.3. Investigation of Genetic Response to Pressure in B. subtilis through RNAseq Technique

RNAseq is a technique that can be used to investigate the quantity and sequences of mRNA in a sample at a particular condition using next-generation sequencing technology. Through this technique, all mRNA sequences in one cell state can be analysed as a transcriptome, to measure the extent to which the genes are expressed.

RNAseq was used to investigate the genetic response to pressure in *B. subtilis*. *B. subtilis* cells were grown in 2% (w/v) LB agarose hydrogel at 37 °C as a 3D culture. When the growth reached the exponential stage, the agarose hydrogels were placed in a customised pressure vessel and treated with either 200 kPa or 400 kPa for 30 min at 37 °C. After the pressure treatment, the cells were immediately frozen in liquid nitrogen and the mRNA was extracted and prepared for RNAseq using TRIzol reagent and a Qiagen RNeasy Plant Mini Kit (QRMP). An RNA analysis was then performed using a Bioanalyser with the HS analysis kit. The *B. subtilis* grown in 3D culture without pressure treatment was used as a control sample and the experiments were performed in four biological replicates and four technical replicates spanning each of the conditions to achieve significant results. RNA samples were sent for sequencing using Illumina HiSeq with 5–10 million reads per sample. In the control, the mix was also added to samples to allow for the creation of a standard baseline measurement of RNA both within this experiment and across other experiments performed using various samples and platforms.

The RNA sequencing data generated from the sequencing were normalised using the ERCC (External RNA Controls Consortium) RNA spike-in controls and fold change (FC) calculated in comparison to the 0 kPa pressure control. Overall, there were 28 and 88 genes that displayed a significant increase in expression with a cut-off of FC $\geq$ 2 for 200 kPa and 400 kPa, respectively. Of these, 18 were common to both conditions suggesting a partially shared response to the increased pressure environment.

To demonstrate this system, a practical bio-geotechnical numerical model of a pressure-responsive MICP system is proposed. This two-dimensional model accounts for varying geotechnical conditions, anisotropic soil permeability, bacteria cell distribution and bacteria genetic response to predict the distribution of calcium carbonate precipitation and the

associated reduction in permeability. Cementation scenarios are presented for different soil conditions resulting from the real genetic responses of selected bacteria which were tested in the lab. In addition, to demonstrate to design potential of this system, the cementation response from an ideal hypothetical engineered bacterium is also presented.

3. Materials and Methods

3.1. Biological Data Collection

There are several sets of biological data required to establish the 2D model. These include bacterial distribution and enzyme activity. In the absence of the high ureolytic *B. subtilis* strain, the experiments were set up using the well-studied MICP bacterium *Sporosarcina pasteurii* which will produce the optimised value. However, one of the objectives of this research is to engineer a pressure-responsive *B. subtilis* strain which has a similar level of enzyme activity through genetic manipulation. There are several strategies which can be applied to achieve this goal, including optimising the translation initiation region sequence [34] or employing a secondary over-expression promoter which is regulated by the protein induced by elevated pressure.

3.1.1. Bacteria Distribution

Bacteria distribution data were collected using sand columns. All experiments were conducted with technical triplicates. Syringes (100 mm length, 25.585 mm ID) were used to facilitate column experiments. A filter paper (2.5 µm particle retention) and cotton layer were positioned at each end of the syringes, and sand (50.9 g) was packed in between these layers. A rubber stopper was used to plug the syringe, and tubing (3 mm internal diameter, 5 mm external diameter) was connected to each end to facilitate the input and output of solutions which were pumped using a peristaltic tubing pump (CTP100, Fisher Scientific, Loughborough, UK) up through the sample from the bottom of the tube. *S. pasteurii* was grown to early stationary phase growth and pumped (1.5 pore volumes (PVs)) upwards into syringes and left undrained for 24 h. Following this, cementation media (3 g L^{-1} nutrient broth (NB), 187 mM NH_4Cl, 333 mM urea, 250 mM $CaCl_2$) were applied to syringes every 24 h for a total of 12 applications. Three syringes were sampled 24 h after each application of cementation media as well as 24 h after the application of *S. pasteurii*. Before sampling, syringes were flushed with 1.5 PVs of 18.2 MΩ·cm H_2O, then were cut into the top, middle and bottom sections (2.5 cm height). From each section, 1 g of sample was taken and suspended in 800 µL 2.5% PEG (polyethylene glycol) 5000 and shaken on a vortex at maximum speed using a microcentrifuge attachment for 1 h. Following this, samples were centrifuged at 950× *g* for 15 min to pellet sand. Inoculate (100 µL) was serially diluted in 18.2 MΩ·cm of H_2O to 10^{-1} and 10^{-2} dilutions, which were spread onto 1.5% NB (13 g L^{-1}) of agar supplemented with 333 mM of urea in duplicate. Plates were incubated at 30 °C for 42 h. Following incubation, plates were checked for colonies. Colony forming units (CFUs) were calculated using the following equation:

$$\text{Colony forming units mL}^{-1} = (\text{colonies number} \times \text{dilution factor})/\text{sample volume (mL)} \quad (7)$$

For the model, only peak values obtained for top column sections were used. The determined concentrations likely represent an underestimation, as not all bacteria may detach from the sand into the solution. However, this error is assumed to be negligible.

3.1.2. Urease Activity at a Cellular Level

The MICP method is based on the process of microbially released urease catalysing the hydrolysis of urea, and the activity of the urease is critical in determining the rate of reaction, i.e., the stabilising effects of the MICP method; therefore, an understanding of the urease activity is required at the laboratory stage, as introduced afterwards. The cultures of *S. pasteurii* were grown to the early stationary phase. The cultures were centrifuged at 18,516× *g* for 15 min at 4 °C and the supernatant was discarded. Cell pellets were washed 3 times in phosphate-buffered saline and final cell pellets were resuspended in 3 g L^{-1}

of NB and 187 mM of NH_4Cl to give an OD_{600} of ~1.0. Cells were then diluted 1:10 into solutions containing 3 g L^{-1} of NB, 187 mM of NH_4Cl and different concentrations of urea (0–1 M). Solutions were incubated at 30 °C and 150 RPM. Conductivity measurements were taken at 0 h, 1 h, 2 h and ~18 h. It was assumed that the reaction rate was linear during the first hour based on the results of [35]. Two biological and two technical replicates were carried out for each solution.

3.2. Model of the Study

3.2.1. Model Domain

The model domain is a plane of 60 m × 30 m, divided into 7200 4-noded rectangular 2D elements, each 0.5 m × 0.5 m. A vertical pressure of 1000 kN/m^2 is applied over a 10 m width at the surface of the soil to simulate construction loading. This model domain is shown in Figure 1. This domain can be assumed to extend infinitely in the y dimension.

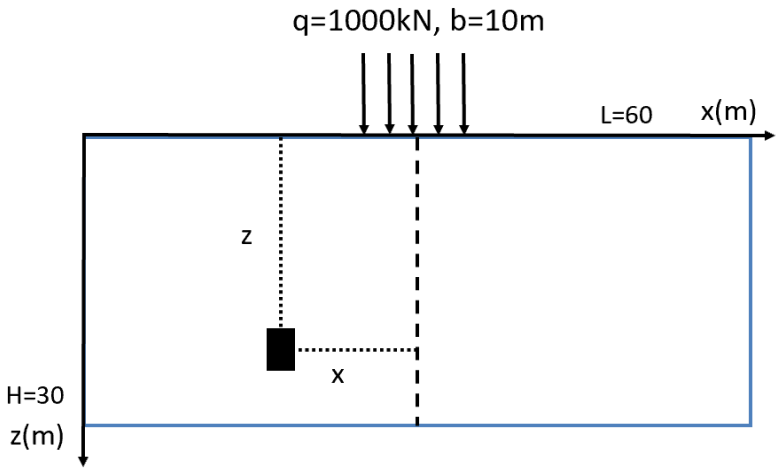

Figure 1. Sketch diagram of the calculation domain.

3.2.2. Geotechnical Theory

An infinitely long strip load on the surface of a semi-infinite elastomer can be simplified as a two-dimensional planar problem, as shown in Figure 1. The additional vertical stress at any point in the soil, due to the applied load, can then be calculated using Flamant solutions, as shown in Equation (8).

$$\sigma_z = P \times \frac{1}{\pi}\left[\tan^{-1}\frac{1-2n}{2m} + \tan^{-1}\frac{1+2n}{2m} - \frac{4m\left(4n^2-4m^2-1\right)}{\left(4n^2+4m^2-1\right)^2+16m^2}\right] \quad (8)$$

where $m = z/b$, $n = x/b$ and x, z and b are shown in Figure 1.

This load is resisted entirely by the water in the saturated soil at the moment of its application, which induces excess pore water pressure [36] above the hydrostatic pore water pressure present initially. The excess pore water pressure (U) at any point in the soil after a given time (t) of consolidation in a 2D domain can then be obtained by solving Equation (9) below, and the static pore water pressure will be added as a constant term in the model calculation, determined by the depth of the domain:

$$\frac{\partial U}{\partial t} = c_x\frac{\partial^2 U}{\partial x^2} + c_z\frac{\partial^2 U}{\partial z^2} \quad (9)$$

where c_x and c_z are the coefficients of consolidation in the horizontal and vertical directions, respectively, and can be calculated as follows:

$$c_x = \frac{k_x(t)}{\gamma_w m_v};\ c_z = \frac{k_z(t)}{\gamma_w m_v} \quad (10)$$

where $k_x(t)$ and $k_z(t)$ are the permeability of the soil in the horizontal and vertical direction and γ_w is the unit weight of water. Previous studies [14,37] have shown that calcium carbonate precipitation results in the reduction in porosity and permeability of the soil. Therefore, horizontal and vertical permeability vary with time. It is worth mentioning that the coefficient of volume change (m_v) is assumed to be a constant in this study.

3.2.3. Calculation Process

The calculation process in the model is shown in Figure 2. Once the pore water pressure in the soil is calculated from theory, three types of experimental data are used to derive the amount of calcium carbonate precipitated in every element in the model domain and the resultant soil permeability in each element. These data will be described in the following sections.

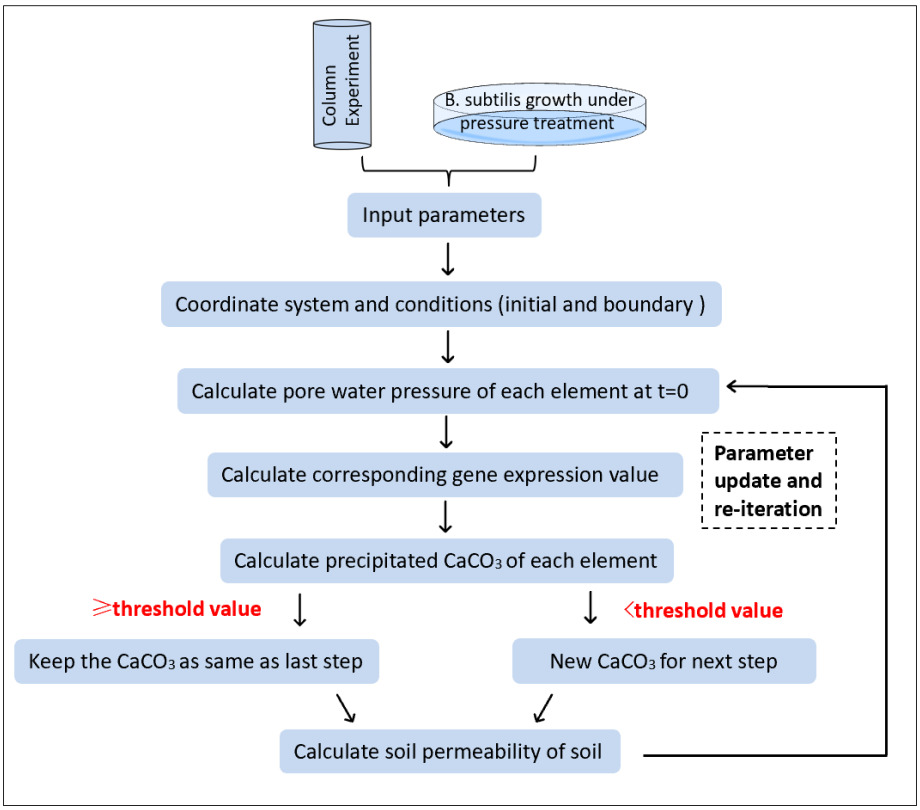

Figure 2. The calculation process of the model used in the study.

3.2.4. Gene Expression Value and Urea Hydrolysis Rate

Using the RNAseq experiments, described above, three genes responding which exhibited significant changes in expression when the pressure was increased from zero to either 200 kPa or 400 kPa were identified and used as model data. The gene expression response data for these three genes are shown in Figure 3. Although there are relatively few data points, curves have been fitted and the dashed lines show a proposed continuation of the behaviour trend for each gene. These projections are not verified but give us a starting point to understand the likely effects of different expression profiles. The genes were selected because they showed a clear response to pressure changes, and each represents a different profile: increasing (Gene A) and decreasing (Gene C) in response to pressure and sensitivity to a particular pressure range (Gene B).

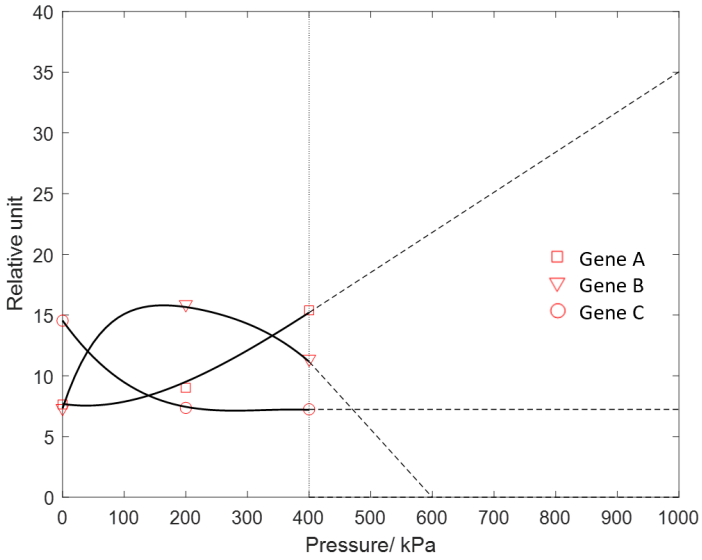

Figure 3. Gene expression data and proposed behaviour for three pressure-responding genes (the x-axis represents the pressures applied to the samples and the y-axis is a relative unit compared to the ERCC ExFold RNA Spike baseline in sequencing control).

In our proposed engineered system, the pressure-sensing promoter gene will be linked to the production of urease, which is subsequentially responsible for inducing calcium carbonate formation in the soil. The calcium carbonate precipitation per unit time can be calculated from the urea hydrolysis rate of the bacteria. Here, to evaluate the influence of different gene expression relationships on the simulation results, we assume the maximum gene expression level as shown in Figure 3 (34.5) produces the maximum urease activity, which is measured in Section 3.1.2. This assumption allows the urea hydrolysis rate corresponding to different gene expressions to be calculated. Noting that here, the fitting curves may not reflect the real relationships due to the lack of data points for higher pressures, the proposed relationships are used for the preliminary exploration of the model. More investigations should be conducted in the future to quantify the relationship between gene expression and the proposed engineered system.

The calcium carbonate precipitation rate is influenced not only by the rate of urea hydrolysis, which is controlled by the gene expression, but also by the bacteria cell distribution in the soil. It is assumed that the concentration of bacteria exhibits an exponential reduction along with soil depth [38]. The number of bacteria cells at the top of the soil has been measured in Section 3.1.1, and then by applying this relationship, the bacteria distribution in the soil will be calculated in-depth. In the horizontal direction, the bacteria distribution is assumed to be homogeneous.

Previous studies on MICP modelling have shown that the simulation can be improved by experimental data [39]. Experiments with *S. pasteurii* for soil improvement have been set up at a small scale in the lab allowing us to investigate the bacterial cell distribution and ureolysis rate. The number of bacteria cells at the top of the soil column has been measured in CFUs as 9×10^4 per gram of soil. The relationship mentioned in [38] is utilised here to calculate the bacteria distribution and Figure 4 shows the majority of bacteria only present in the top 10 m of soil. It is worth mentioning that here, the bacteria distribution in Soil 2 and Soil 3 are assumed in accordance with this relationship as well.

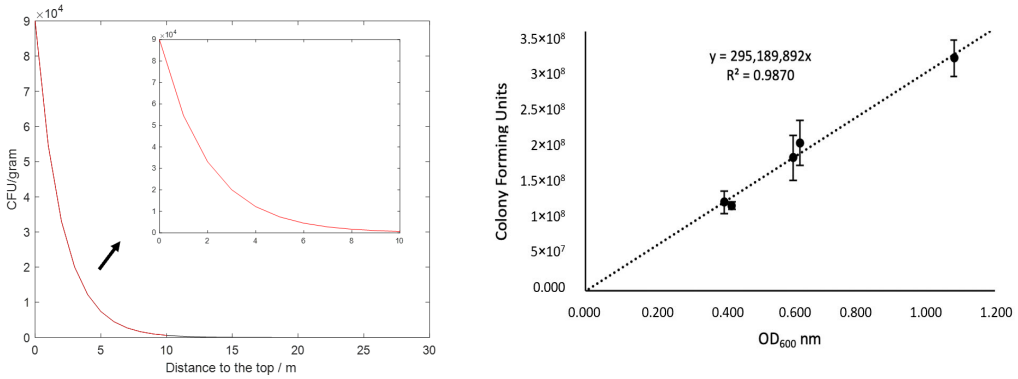

(**a**) (**b**)

Figure 4. Bacteria test results: (**a**) Bacteria distribution in the model domain; (**b**) *S. pasteurii* DSM 33 colony forming units plotted against different OD600 values.

To calculate the rate of urea hydrolysis, the peak rate—which occurs at the point of urease saturation—was used to calculate the rate which was 1310.96 mM per hour per OD_{600}. This was converted to a per-cell rate using a standard curve showing a relationship between CFUs and OD_{600}, to give a final urea hydrolysis rate of 1.03×10^{-6} mM per CFU per hour. In the model, we assume the maximum gene expression level produces the maximum urease activity. This assumption allows the urea hydrolysis rate corresponding to different gene expressions to be calculated.

3.2.5. Calcium Carbonate Production and Influence on Permeability

The amount of calcium carbonate precipitation per unit of time at a given point can be calculated by multiplying the bacteria number by the mass of soil in the element and the urea hydrolysis rate. It is assumed that calcium carbonate is formed in the pores of the soil. As the volume of pores in a given soil is limited, no further precipitation will occur once this volume is filled. This upper limit value can be calculated by the porosity of the soil and density of the calcium carbonate as follows.

Taking Soil 1 as an example, for each element in the domain, assuming the length in the y direction of the element is also 0.5 m and based on the data in Table 1, the volume of the element, the soil mass in the element and the void space in the element can be calculated as follows:

$$V_{\text{elememt}} = 0.5 \times 0.5 \times 0.5 = 0.125\ \text{m}^3 = 1.25 \times 10^5\ \text{cm}^3$$
$$m_{\text{element}} = 125000 \times 1.76 = 2.2 \times 10^5\ \text{g}$$
$$V_{\text{void}} = 125000 \times 0.34 = 4.25 \times 10^4\ \text{cm}^3$$

For each soil, the maximum mass of calcium carbonate in an element in the model is shown in Table 1.

Table 1. Material properties.

Property	Soil 1	Soil 2	Soil 3
Initial permeability in x direction k_x (m/s) *1	2.25×10^{-4}	7.5×10^{-6}	6×10^{-8}
Initial permeability in z direction k_z (m/s) *1	1.5×10^{-4}	5×10^{-6}	4×10^{-8}
Average coefficient of volume change m_v (kPa^{-1}) *1	3×10^{-4}	4.5×10^{-4}	6×10^{-4}
Bulk density ρ_{bulk} (g/cm^3) *1	1.76	1.60	1.50
Initial porosity *1	0.34	0.4	0.50
British Standard Classification *2	SM	Silt	CL
Maximum mass of calcium carbonate per element (g)	115,175	135,500	169,375
Bacteria concentration at the top of soil (CFU/g) *3		8.64×10^4	
$CaCO_3$ precipitation rate (mM/CFU/hour) *3		1.03×10^{-6}	
Density of the calcium carbonate (g/cm^3) *4		2.71	

*1 Results in ref. [40]. *2 BSI Standard [41]. *3 Results in ref. [42]. *4 Results in ref. [43].

As calcium carbonate is precipitated and fills the pore space, it causes a reduction in the porosity and permeability of the soil. This variation in the permeability also influences the rate of pore water pressure dissipation in both x and z directions, so this is included in the model. Figure 5 shows data from previous studies on the influence of the calcium carbonate content ratio (gravimetric content to the dry soil) on the permeability of the fine sand/silty sand soils. A fitting curve is introduced to describe a general trend of these results and this relationship is used for all soils in this study.

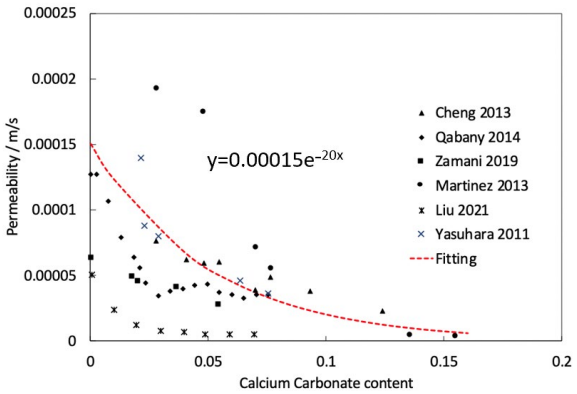

Figure 5. Relationships between gravimetric calcium carbonate content and permeability of sand in previous studies [8,26,44–47].

Three soils are used in the model, with properties as shown in Table 1. The coefficient of volume change (m_v) changes with pressure; however, an average value is adopted. Soil 1 is a silty sand used for the laboratory tests of bio-cementation described in Section 3.2.5 Bacteria Distribution. To assess the performance of the pressure-responsive MICP system in realistic geotechnical scenarios, two other soils have also been considered: silt (Soil 2) and low-plasticity clay (Soil 3), with properties as shown in Table 1. Experimental results for the bacteria concentration at the top of sand samples are also included in Table 1.

3.2.6. Further Assumptions

As well as those discussed so far, the model is based on the following assumptions:

(1) Calcium carbonate is only present in the solid phase and not transported.
(2) The urea and calcium solution does not influence the permeability of the soil.
(3) Bacteria are immobile and do not influence the porosity of the soil and the uniformity of precipitation.
(4) Each layer of soil is homogenous and fully saturated.
(5) Urea and calcium are at the same concentration, and both react at the same rate.
(6) All boundaries of the model are fully permeable and pore pressures at these boundaries are always zero.

3.3. Material Properties

Two soil profiles are used in the model. The first of these is a homogeneous clay layer, to simulate an area with thick clay deposits (e.g., London Clay), as shown in Figure 6a. This condition also demonstrates the behaviour of the responsive cementation system in a relatively simple scenario where high pore pressures are maintained due to the low permeability of the soil, allowing maximum cementation to occur. The properties of the clay in this profile are shown in Table 1. The second profile is established based on the typical scenario of cases in the available literature [48–50] and consists of six layers of soils of varying permeability, as shown in Figure 6b, and with properties shown in Table 1. Two represented points (A and B) are also shown in Figure 6; they are selected by considering a typical weak soft clay layer under surcharge and the bearing strata of pile

foundation, respectively; they will be discussed in the following section. Results from these points will be used to compare how different gene responses affect cementation behaviour.

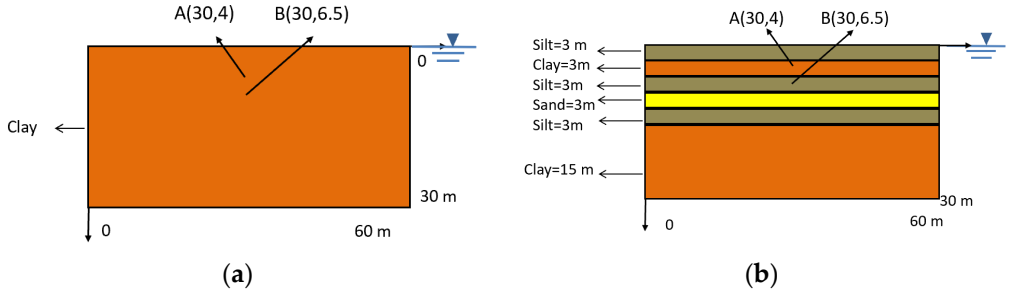

Figure 6. Soil layer distribution in this study: (**a**) soil profile 1; (**b**) soil profile 2.

4. Results

4.1. Experimental Genes

Results are presented from modelling the behaviour of the pressure-responsive cementation system in the two soil profiles mentioned above. The outcomes from three existing pressure-responsive genes are presented, along with three idealised hypothetical gene responses to demonstrate how synthetic biology can be used to design these responses and achieve more favourable outcomes. The calcium carbonate distribution over time in soil profile 1 (homogeneous clay), due to the response of Gene A, Gene B and Gene C, are shown in Figures 7–9, respectively.

Figures 7–9 demonstrate the different distributions of cementation that can be achieved by different genes in soil profile 1. In the 7-day consolidation, Genes A and B tend to produce $CaCO_3$ at the centre area just beneath the ground surface and broaden out to a larger area, finally producing a concentration of cementation in the centre and non-centre areas, respectively. Gene C has laterally uniform precipitation but without a centre area initially and develops the precipitation to the deeper area. The cementation distribution over time in soil profile 2, due to the response of three genes, are shown in Figures 10–12, respectively. During the process of consolidation, the first layer of the domain (0–3 m) is gradually filled with $CaCO_3$ for all three genes. In addition, $CaCO_3$ can be found in the centre area, centre-surrounded area and non-centre area of the second layer (4–6 m) initially in Genes A (Figure 10b), B (Figure 11b) and C (Figure 12b). Then, the precipitation in the areas mentioned above develops gradually to different degrees.

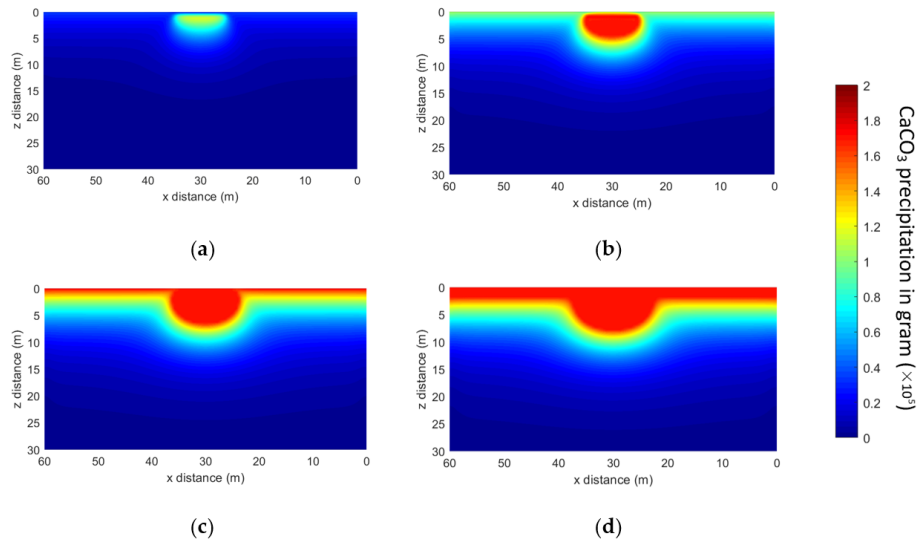

Figure 7. Calcium carbonate precipitation distribution in soil profile 1 due to the Gene A after (**a**) 1 day; (**b**) 3 days; (**c**) 5 days; (**d**) 7 days.

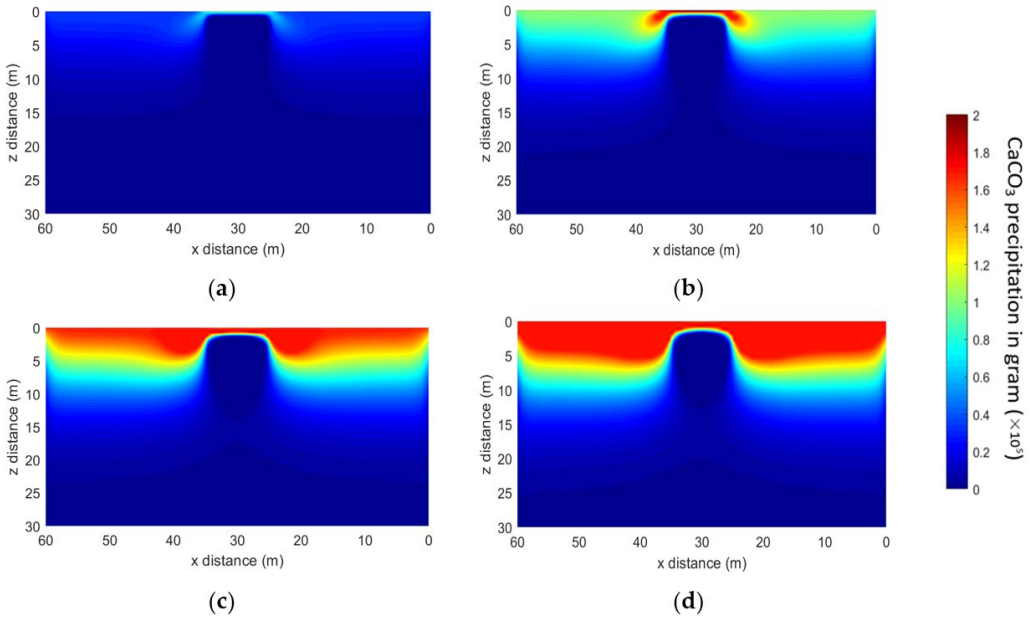

Figure 8. Calcium carbonate precipitation distribution in soil profile 1 due to the Gene B after (**a**) 1 day; (**b**) 3 days; (**c**) 5 days; (**d**) 7 days.

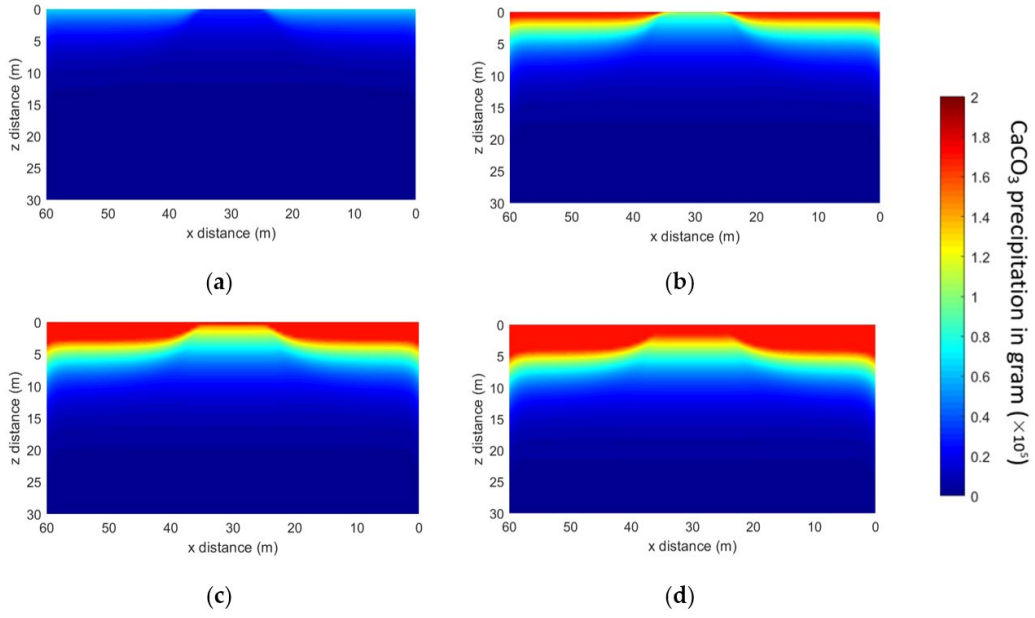

Figure 9. Calcium carbonate precipitation distribution in soil profile 1 due to the Gene C after (**a**) 1 day; (**b**) 3 days; (**c**) 5 days; (**d**) 7 days.

By combining the trends in the simulation results above, it can be found that for the given soil profile, a system with Gene A tends to have the highest precipitation quantity in the middle area (beneath the place where the load is applied) of the domain, which can contribute a good effect in declining the settlement of this area; a system with Genes B and C has a greater "core area" with a high value of $CaCO_3$ in the domain laterally and vertically, but a lack of precipitation in the middle. Hence, these two genes could be used for stabilising projects built on weak soils or with existing constructions surrounded. For the same gene, in both soil profiles 1 and 2, the cementation is confined to the top 10 m of the soil layer, due to the reduction in bacteria numbers at the greater depths. Compared with soil profile 1, the cementation distribution pattern in soil profile 2 is more complex due to the different characteristics of strata, and the greatest precipitation is concentrated

in the area of the second layer (4–6 m in depth) for all gene types, because the pore water pressure in this layer can maintain a relatively high value for a longer time.

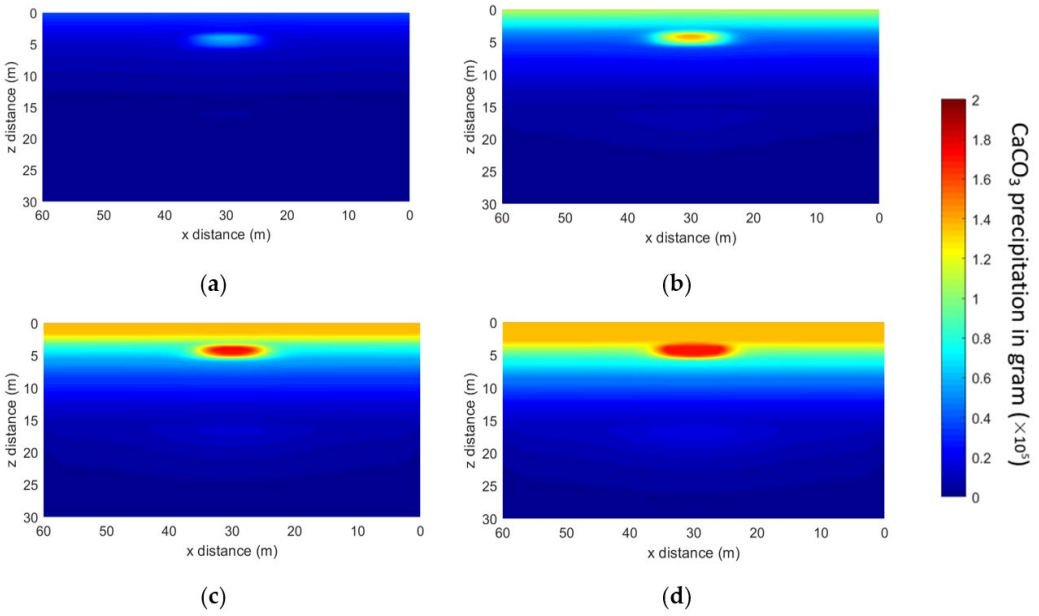

Figure 10. Calcium carbonate precipitation distribution in soil profile 2 due to the system with Gene A gene after (**a**) 1 day; (**b**) 3 days; (**c**) 5 days; (**d**) 7 days.

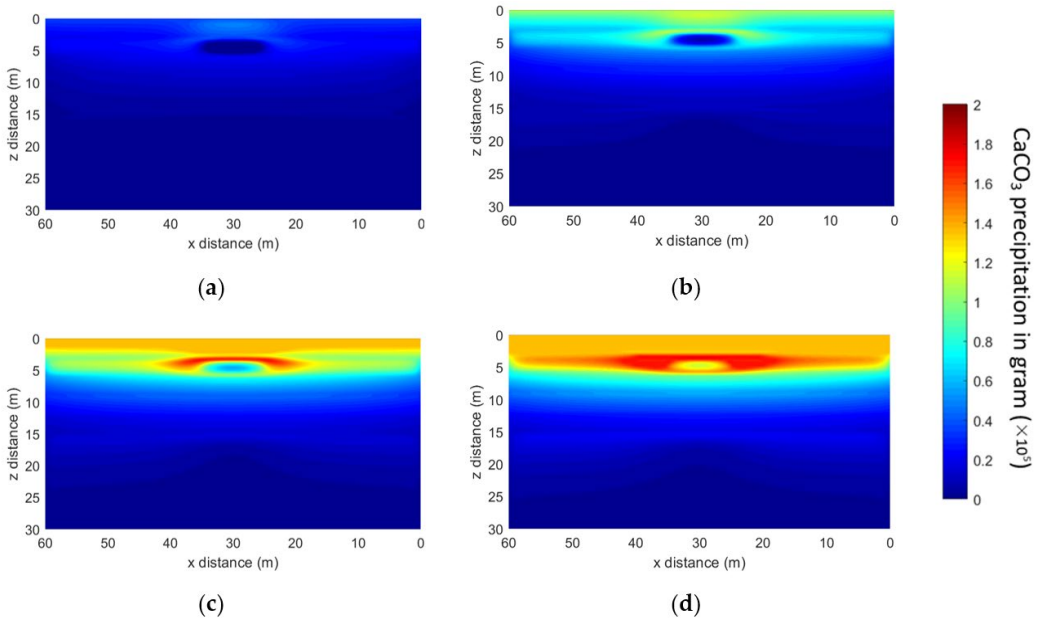

Figure 11. Calcium carbonate precipitation distribution in soil profile 2 due to the system with Gene B after (**a**) 1 day; (**b**) 3 days; (**c**) 5 days; (**d**) 7 days.

Further, precipitation of points A and B (as mentioned above) in different genes and soil profiles are shown in Figure 13. It can be seen that in soil profile 1 (Figure 13a), a system with Gene A has the quickest response, and the maximum value of precipitation at points A and B; lower precipitation and no calcium carbonate have been found in Genes C and B, respectively, because the pore water pressure in these points is too low/high for these two gene relationships. As for soil profile 2 (Figure 13b), in point A, a system with Genes A and B reaches the maximum value at different rates, while Gene C does not. In point B, the material in this layer leads to a relatively low pore water pressure, so Gene C

has the greatest precipitation rate because the gene expression has a negative correlation with pressure in the range of 0–200 kPa. It can be concluded that in point A, a system with Gene A has the highest precipitation value and rate in both soil profiles, then followed by Gene C and Gene B. As for point B, Gene C has the best performance by combining both soil profiles, followed by Gene A and Gene B. As mentioned above, the depth of point A represents a typical soft clay layer under the bearing strata, so it can be deduced that Gene A has the best stabilisation effect in reducing the settlement of shallow soft clay strata under load. Point B can be seen as a potential location of bearing strata of piles; hence, one can conclude that Gene C is the most suitable gene for stabilising the pile foundation.

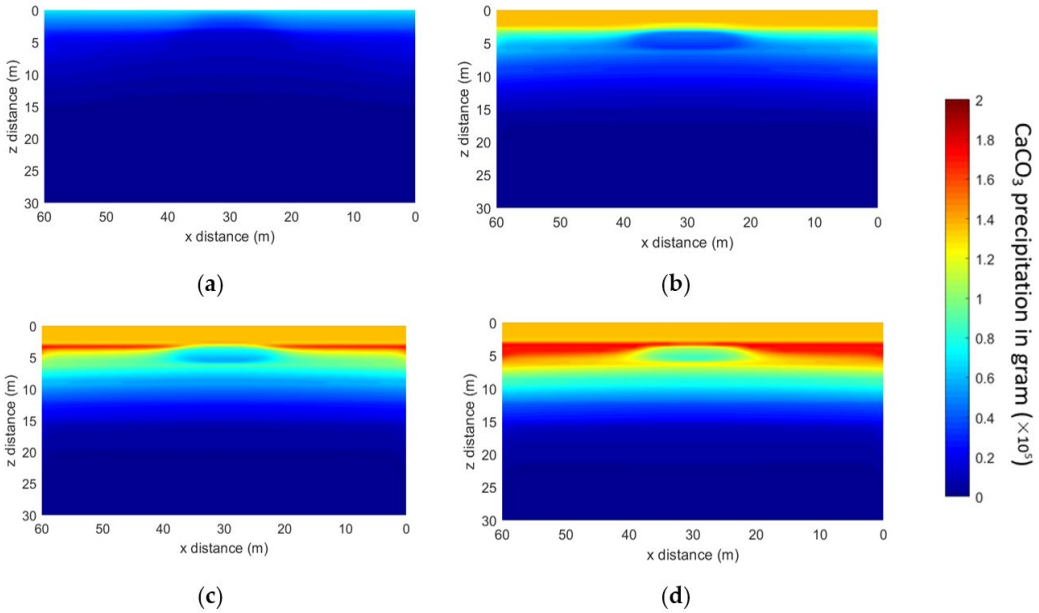

Figure 12. Calcium carbonate precipitation distribution in soil profile 2 due to the system with Gene C gene after (**a**) 1 day; (**b**) 3 days; (**c**) 5 days; (**d**) 7 days.

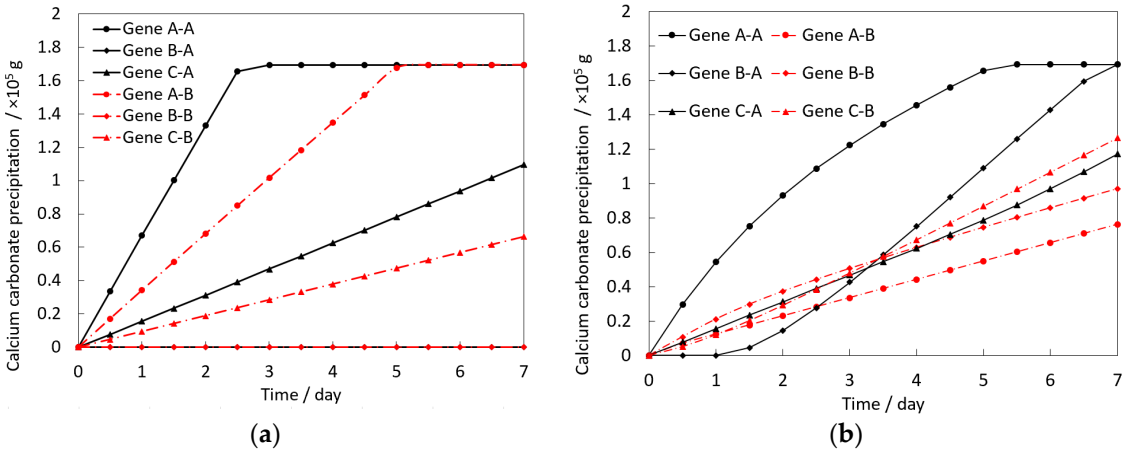

Figure 13. Variation of calcium carbonate precipitation with time at points A and B in (**a**) soil profile 1; and (**b**) soil profile 2.

Combining the precipitation patterns and typical points in both soil profiles, it can be understood that for the strata immediately beneath the ground surface (z = 1 m), there is no significant difference among the tested genes in precipitation value after 7 days. Hence, all three genes are capable of applications considering shallow treatment depth (e.g., road embankment). If the stabilisation rate is considered, Gene A and Gene C are the most suitable for soil profiles 1 and 2, respectively, due to the strong effect in the early stage

of the reaction. As the strata goes deeper (2–5 m), it can be concluded that Gene A is most suitable for the stabilisation for most applications (e.g., shallow foundation), as the stress and settlement in the centre area are the most significant, Genes B and C might be employed when the settlement of the surrounded existing structure is the top priority consideration. For further depth (>6 m), all three genes have much less precipitation as the bacteria number declines sharply. In soil profile 1, Gene A and Gene C have a better effect in stabilising the centre and edge areas, respectively. In soil profile 2, Gene C has the best behaviour with homogenous precipitation laterally. These two genes can be utilised according to the geology conditions when the deeper area of soil needs to be stabilised (e.g., deep foundation).

4.2. Hypothetical Genes

The above results show that all three genes can stabilise soil foundations to various extents; however, in the engineering world, the tested genes are inefficient because usually only the specific area in the foundation needs stabilisation. Hence, targeted stabilisation would need to be realised using bespoke gene promotors to suit specific geotechnical contexts. Such hypothetical genes can be simulated and tested as part of the synthetic biology design process. Therefore, the model is envisaged as part of the synthetic biology design cycle. Using the data above, we can, therefore, begin to design such a system. In the proposed system, the implementation of a biological logic gate is suggested. In our natural pressure-sensitive genes, a varying relationship to pressure is observed. By engineering the cells, one can distinguish between different logical operations in response to a stimulus. In this case, a gene response is designed which is proportionally responsible to the stimulus such that as pressure subsides, gene activity does as well.

In Figure 14, the expression of a hypothetical gene called D is shown; it can be seen that the gene does not respond to pressure until it increases to a threshold value of 200 kPa, after which the gene remains "switched on" and a constant rate of expression of 1.03×10^{-6} mM/CFU/hour is employed. We also test two further hypothetical constructs, Genes F and G, with threshold values of 400 and 600 kPa. The calcium carbonate precipitation after 7 days due to Genes D, E and F in different soil profiles are shown in Figure 15.

This system has several advantages, which are explained as follows. Firstly, the pressure switch is activated at a threshold value and its status will not switch off after pressure within the soils diminishes leading to the maintenance of high levels of urease activity. We know, for example, that in sandy soils, water pressure drops quickly as water escapes the open pores between sand grains. However, sandy soils are also likely to be in the most need of soil improvement. Assuming that the genetic switch can operate fast enough, the water pressure beneath the applied load, therefore, does not need to stay high for long to trigger the cementation process [51,52].

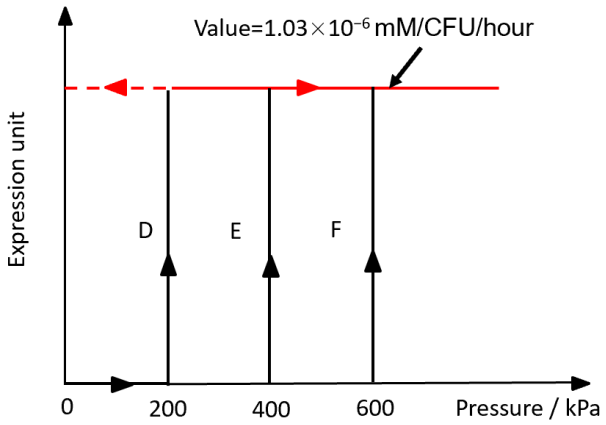

Figure 14. Hypothetical gene relationships in this study.

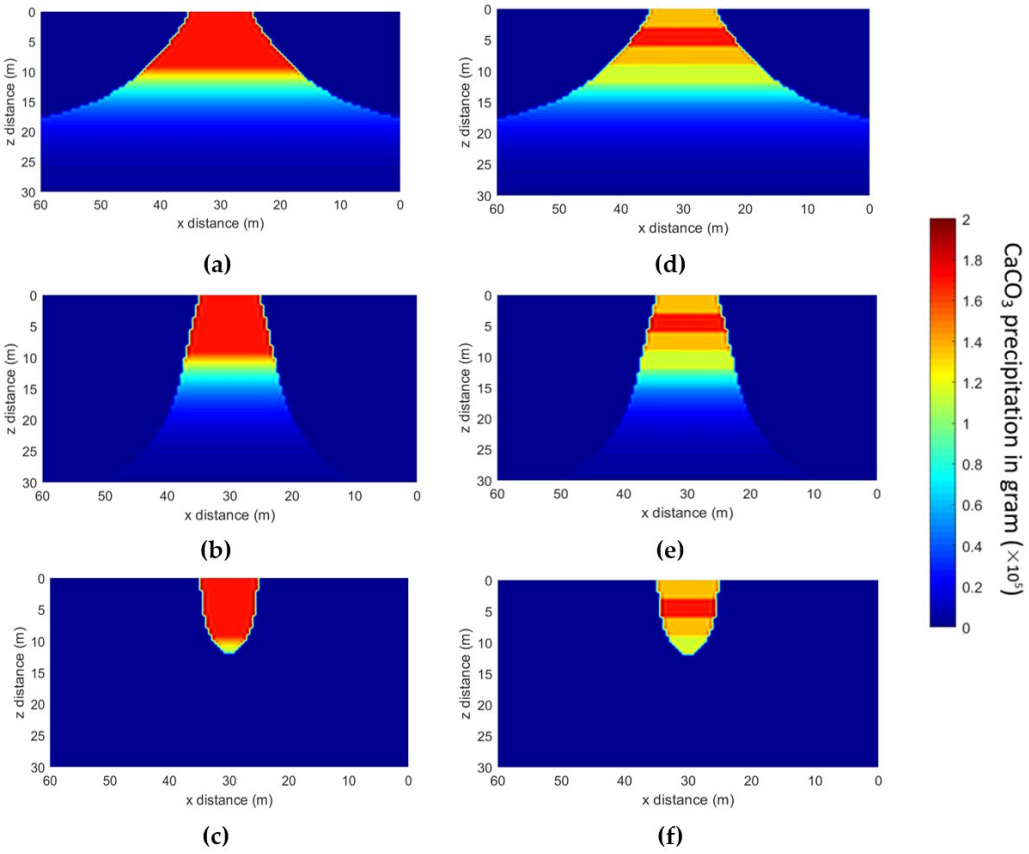

Figure 15. Calcium carbonate precipitation after 7 days due to the system with hypothetical genes: (**a**–**c**) Genes D, E and F in soil profile 1; (**d**–**f**) Genes D, E and F in soil profile 2.

Secondly, when a certain reinforced area is needed in multi-layer conditions, the stabilisation in this method can be more accurate by controlling the threshold value of gene expression and injection time. For example, for the soil profile with drained materials (e.g., sandy soil) at the upper layers and firm soil (e.g., silty clay) as the bearing stratum at the lower layers, the latter soil which holds the piles needs to be stabilised, but the former does not. Soon after the soil consolidation, the pore water pressure dissipates in the upper layers for a short period but remains for a period (depending on the soil condition) in the lower layers. Consequently, one can use the designed gene with a threshold value relative to the kept pore water pressure and inject it after a short period of consolidation to make the $CaCO_3$ precipitation occur only in the bearing stratum.

Finally, for the complex engineering projects with different positions to be stabilised to different degrees, two or more types of synthetic genes with different threshold values can be utilised and injected into the different matched positions, respectively; this can ensure the needed positions are stabilised with different rates and to the target degrees eventually. Based on the synthetic biology method, the soil stabilisation patterns in the three hypothetical cases mentioned above are efficient and economical, compared with the experimental genes, so it can be concluded that the synthetic genes have the potential to be used in different working conditions with a better stabilisation effect. However, the conclusions above are based on a highly idealised model and cannot completely reflect the situation of the real engineering world due to the limitations of the test data. Hence, further investigations are needed on this and model simulations for the different synthetic genes under different working conditions. Real-world experimental data on this are also likely to be important as there are many complex factors involving the sociability of the engineered bacteria when competing with other species and in non-optimised conditions of nutrient availability and temperature, etc.

5. Conclusions

In this study, a novel computational model is designed to demonstrate a pressure-responsive calcium carbonate precipitation system. Results are presented showing the system's performance in the context of two different soil profiles, with three laboratory genes and three hypothetical genes. The results from this study are highly preliminary and based on early lab data and assumptions which are likely to be challenged as new experimental data emerge. Nonetheless, the model can be seen as a framework for simulating biological improvements across scales with Engineered Microorganisms. This study conducted with the model is also an example of a design process, in which gene expression is considered a key factor to the success of different soil improvement strategies. Consequently, one can glean valuable insights from the results and the utility of this model, as outlined below:

(1) Genes with different expression profiles have a significant influence on the precipitation patterns and relevance to different geotechnical contexts, in both soil profiles. For example, Gene A shows a quicker transcriptional response in the area under the applied stress, which might be the weakest part of the application, and finishes with a better stabilisation effect in this area. Gene C shows the best effect in reinforcing the edge area and has the greatest influenced depth. It can be used in stabilising foundations with existing surrounding structures or in the deeper underground area, e.g., the pile foundation.

(2) The soil profile, therefore, also influences precipitation results. Homogeneous clay soil tends to maintain high pore water pressure levels and benefits genes with increasing trend expression (e.g., Gene A). In multi-layer soil conditions, three genes have similar stabilisation results in the top layer and tend to benefit different areas in the lower layers. For any gene, the soil in higher layers tends to have a quicker precipitation rate than in lower layers due to a greater bacteria cell number count.

(3) For a given working condition, the stabilisation area can be adjusted by selecting different genes and the stabilisation effect can be enhanced through the development of biological logic gates as in the 'latched gate' circuit proposed here in which genes are switched on at a threshold pressure value and remain on even after pressure drops. Developing more detailed gene expression data will lead to the possibility of modelling different experimental and synthetic genes under different working conditions and building a gene library to give guidance for gene selection could further research purposes.

The most important simulations described above demonstrate that we can build a model which maps between data on genetic responses from engineered bacteria through to large-scale geotechnical models which describe soils under load. MICP-based soil improvement has already been implemented but our system goes much further by suggesting the development of new biologically engineered systems. The paper described an innovative model to understand how these systems may work. This significantly extends the range of models available in synthetic biology to support the design–simulate–build-test cycle. Our model describes soils as large ELMs, able to be biologically programmed to adapt to their environment. The model also has utility in synthetic biology, where the design of novel organisms is driven by computational modelling. The computational model described here allows us to understand the dynamics of soil loading, elevated water pressures and factors such as microbial distribution to design the appropriate pressure-sensing capability for different geotechnical conditions. It should be recognised that we are still some distance from such an application. Many of the assumptions from which our model is derived are contestable and the actual biological implementation of a pressure-sensing system of this sort will require a deeper knowledge of microbe–soil interactions. It is also worth recognising that applications which require the release of Genetically Modified Organisms (GMOs) into the environment are controversial and will require ethical as well as legal considerations. We have, however, shown that it is possible to map across a range of scales—from the nano-scale gene regulation through to geophysics and meter scales.

Author Contributions: Conceptualisation, M.D.R.; methodology, H.M.; software, J.W.; validation, J.W., H.M. and M.D.R.; formal analysis, J.W.; investigation, J.W.; resources, P.M. and J.H.; data curation, P.M. and J.H.; writing—original draft preparation, J.W., M.D.R. and H.M.; writing—review and editing, M.Z. and A.W.; visualisation, J.W.; supervision, M.D.R.; project administration, M.D.R.; funding acquisition, M.D.R., M.Z. and J.W. All authors have read and agreed to the published version of the manuscript.

Funding: This research was funded by the UK Engineering and Physical Sciences Research Council, grant number EP/N005791/1, EP/R003629/1 and EP/R003777/1 and the National Natural Science Foundation of China, grant number 42202309.

Institutional Review Board Statement: Not applicable.

Informed Consent Statement: Not applicable.

Data Availability Statement: The data presented in this study are available on request from the corresponding author.

Acknowledgments: This work was supported by the UK Engineering and Physical Sciences Research Council and the National Natural Science Foundation of China, which is gratefully acknowledged.

Conflicts of Interest: The authors declare no conflicts of interest.

References

1. Daraei, A.; Herki, B.M.; Sherwani, A.F.H.; Zare, S. Rehabilitation of portal subsidence of heybat sultan twin tunnels: Selection of shotcrete or geogrid alternatives. *Int. J. Geosynth. Ground Eng.* **2018**, *4*, 15. [CrossRef]
2. Gul, N.; Mir, B.A. Performance evaluation of silty soil reinforced with glass fiber and cement kiln dust for subgrade applications. *Constr. Build. Mater.* **2023**, *392*, 131943. [CrossRef]
3. Baldovino, J.A.; Moreira, E.B. Empirical relationships with unconfined compressive strength and split tensile strength for the long term of a lime-treated silty soil. *J. Mater. Civ. Eng.* **2018**, *30*, 06018008. [CrossRef]
4. DeJong, J.T.; Mortensen, B.M. Bio-mediated soil improvement. *Ecol. Eng.* **2010**, *36*, 197–210. [CrossRef]
5. Soon, N.W.; Lee, L.M. Factors affecting improvement in engineering properties of residual soil through microbial-induced calcite precipitation. *J. Geotech. Geoenviron. Eng.* **2014**, *140*, 04014006. [CrossRef]
6. Xu, X.; Guo, H. Bio-cementation improvement via $CaCO_3$ cementation pattern and crystal polymorph: A review. *Constr. Build. Mater.* **2021**, *297*, 123478. [CrossRef]
7. Omoregie, A.I.; Ngu, L.H. Low-cost cultivation of *Sporosarcina pasteurii* strain in food-grade yeast extract medium for microbially induced carbonate precipitation (MICP) application. *Biocatal. Agric. Biotechnol.* **2019**, *17*, 247–255. [CrossRef]
8. Zamani, A.; Montoya, B.M. Permeability reduction due to microbial induced calcite precipitation in sand. In Proceedings of the Geo-Chicago 2016: Sustainability and Resiliency in Geotechnical Engineering, Chicago, IL, USA, 14–18 August 2016; pp. 94–103. [CrossRef]
9. Tiwari, N.; Satyam, N. Micro-mechanical performance evaluation of expansive soil biotreated with indigenous bacteria using MICP method. *Sci. Rep.* **2021**, *11*, 10324. [CrossRef] [PubMed]
10. Lv, C.; Li, W.Q. Characterization and quantification of calcite distribution in MICP-treated sand using μ-XRF image processing technique. *Acta Geotech.* **2024**, *19*, 115–129. [CrossRef]
11. Montoya, B.M.; DeJong, J.T. Stress-strain behavior of sands cemented by microbially induced calcite precipitation. *J. Geotech. Geoenviron. Eng.* **2015**, *141*, 04015019. [CrossRef]
12. Liu, B.; Zhu, C. Bio-remediation of desiccation cracking in clayey soils through microbially induced calcite precipitation (MICP). *Eng. Geol.* **2020**, *264*, 105389. [CrossRef]
13. Fang, X.; Yang, Y. Influence of fiber content and length on engineering properties of MICP-treated coral sand. *Geomicrobiol. J.* **2020**, *37*, 582–594. [CrossRef]
14. Hataf, N.; Baharifard, A. Reducing soil permeability using microbial induced carbonate precipitation (MICP) method: A case study of shiraz landfill soil. *Geomicrobiol. J.* **2020**, *37*, 147–158. [CrossRef]
15. Fu, T.; Saracho, A.C. Microbially induced carbonate precipitation (MICP) for soil strengthening: A comprehensive review. *Biogeotechnics* **2023**, *1*, 100002. [CrossRef]
16. Golovkina, D.A.; Zhurishkina, E.V. Integration of Organic Waste for Soil Stabilization through MICP. *Appl. Sci.* **2023**, *14*, 62. [CrossRef]
17. Tian, Y.; Li, Z. Application of MICP in water stability and hydraulic erosion control of phosphogypsum material in slope. *Appl. Sci.* **2022**, *12*, 1783. [CrossRef]
18. Gomez, M.G.; Martinez, B.C. Field-scale bio-cementation tests to improve sands. *Proc. Inst. Civ. Eng. Ground Improv.* **2015**, *168*, 206–216. [CrossRef]
19. Meng, H.; Gao, Y. Microbially induced carbonate precipitation for wind erosion control of desert soil: Field-scale tests. *Geoderma* **2021**, *383*, 114723. [CrossRef]

20. Van Wijngaarden, W.K.; Vermolen, F.J. Modelling biogrout: A new ground improvement method based on microbial-induced carbonate precipitation. *Transp. Porous Media* **2011**, *87*, 397–420. [CrossRef]
21. Van Wijngaarden, W.K.; Van Paassen, L.A. A reactive transport model for biogrout compared to experimental data. *Transp. Porous Media* **2016**, *111*, 627–648. [CrossRef]
22. Martinez, B.C.; DeJong, J.T. Bio-geochemical reactive transport modeling of microbial induced calcite precipitation to predict the treatment of sand in one-dimensional flow. *Comput. Geotech.* **2014**, *58*, 1–13. [CrossRef]
23. Wang, X.; Nackenhorst, U. A coupled bio-chemo-hydraulic model to predict porosity and permeability reduction during microbially induced calcite precipitation. *Adv. Water Resour.* **2020**, *140*, 103563. [CrossRef]
24. Wang, J.; Long, Y. Numerical Simulation of Forming MICP Horizontal Seepage Reducing Body in Confined Aquifer for Deep Excavation. *Appl. Sci.* **2023**, *13*, 601. [CrossRef]
25. DeJong, J.T.; Soga, K. Biogeochemical processes and geotechnical applications: Progress, opportunities and challenges. *Géotechnique* **2013**, *63*, 287–301. [CrossRef]
26. Liu, K.W.; Jiang, N.J. An experimental study of mitigating coastal sand dune erosion by microbial-and enzymatic-induced carbonate precipitation. *Acta Geotech.* **2021**, *16*, 467–480. [CrossRef]
27. Duraisamy, Y.; Airey, D.W. Performance of biocemented Sydney sand using ex situ mixing technique. *DFI J. J. Deep Found. Inst.* **2015**, *9*, 48–56. [CrossRef]
28. Bu, C.; Lu, X. Soil improvement by microbially induced calcite precipitation (MICP): A review about mineralization mechanism, factors, and soil properties. *Arab. J. Geosci.* **2022**, *15*, 863. [CrossRef]
29. Mitchell, J.K.; Santamarina, J.C. Biological considerations in geotechnical engineering. *J. Geotech. Geoenviron. Eng.* **2005**, *131*, 1222–1233. [CrossRef]
30. Dade-Robertson, M.; Mitrani, H. Design and modelling of an engineered bacteria-based, pressure-sensitive soil. *Bioinspir. Biomim.* **2018**, *13*, 046004. [CrossRef] [PubMed]
31. Guyet, A.; Dade-Robertson, M. Mild hydrostatic pressure triggers oxidative responses in Escherichia coli. *PLoS ONE* **2018**, *13*, e0200660. [CrossRef]
32. Endy, D. Foundations for engineering biology. *Nature* **2005**, *438*, 449–453. [CrossRef] [PubMed]
33. Crick, F. Central dogma of molecular biology. *Nature* **1970**, *227*, 561–563. [CrossRef] [PubMed]
34. Renning, M.S. Synthetic Biology Approaches for Protein Production Optimization in Bacterial Cell Factories. Ph.D. Thesis, Technical University of Denmark, Copenhagen, Denmark, 2017.
35. Lauchnor, E.G.; Topp, D.M. Whole cell kinetics of ureolysis by *Sporosarcina pasteurii*. *J. Appl. Microbiol.* **2015**, *118*, 1321–1332. [CrossRef] [PubMed]
36. Terzaghi, K. *Theoretical Soil Mechanics*; Wiley: New York, NY, USA, 1943; pp. 265–296. [CrossRef]
37. Lin, H.; Suleiman, M.T. Investigation of pore-scale CaCO3 distributions and their effects on stiffness and permeability of sands treated by microbially induced carbonate precipitation (MICP). *Soils Found.* **2020**, *60*, 944–961. [CrossRef]
38. Barkouki, T.H.; Martinez, B.C. Forward and inverse bio-geochemical modeling of microbially induced calcite precipitation in half-meter column experiments. *Transp. Porous Media* **2011**, *90*, 23–39. [CrossRef]
39. Cunningham, A.B.; Class, H. Field-scale modeling of microbially induced calcite precipitation. *Comput. Geosci.* **2019**, *23*, 399–414. [CrossRef]
40. Carter, M.; Bentley, S.P. *Soil Properties and Their Correlations*; John Wiley & Sons: Hoboken, NJ, USA, 2016.
41. BSI. *Methods of Test for Soils for Civil Engineering Purposes, Part 2: Classification Tests*; BSI Standards Publication: London, UK, 1990.
42. Haystead, J.; Dade-Robertson, M. The investigation of microbial induced calcium carbonate precipitation for soil improvement. *Access Microbiol.* **2020**, *2*, 216. [CrossRef]
43. Mu, Z.; Kong, K. Pressure-driven fusion of amorphous particles into integrated monoliths. *Science* **2021**, *372*, 1466–1470. [CrossRef]
44. Cheng, L.; Cord-Ruwisch, R. Cementation of sand soil by microbially induced calcite precipitation at various degrees of saturation. *Can. Geotech. J.* **2013**, *50*, 81–90. [CrossRef]
45. Qabany, A.A.; Soga, K. Effect of chemical treatment used in MICP on engineering properties of cemented soils. In *Bio-and Chemo-Mechanical Processes in Geotechnical Engineering: Géotechnique Symposium in Print*; ICE Publishing: London, UK, 2014. [CrossRef]
46. Martinez, B.C.; DeJong, J.T. Experimental optimization of microbial-induced carbonate precipitation for soil improvement. *J. Geotech. Geoenviron. Eng.* **2013**, *139*, 587–598. [CrossRef]
47. Yasuhara, H.; Hayashi, K.; Okamura, M. Evolution in mechanical and hydraulic properties of calcite-cemented sand mediated by biocatalyst. In Proceedings of the Geo-Frontiers 2011: Advances in Geotechnical Engineering, Dallas, TX, USA, 13–16 March 2011. [CrossRef]
48. Chai, J.; Ong, C.Y. Lateral displacement under combined vacuum pressure and embankment loading. *Géotechnique* **2013**, *63*, 842–856. [CrossRef]
49. Yamashita, K.; Hamada, J. Seismic behavior of piled raft with ground improvement supporting a base-isolated building on soft ground in Tokyo. *Soils Found.* **2012**, *52*, 1000–1015. [CrossRef]
50. Parsa-Pajouh, A.; Fatahi, B.; Vincent, P.; Khabbaz, H. Trial embankment analysis to predict smear zone characteristics induced by prefabricated vertical drain installation. *Geotech. Geol. Eng.* **2014**, *32*, 1187–1210. [CrossRef]

51. Bradley, R.W.; Buck, M. Recognizing and engineering digital-like logic gates and switches in gene regulatory networks. *Curr. Opin. Microbiol.* **2016**, *33*, 74–82. [CrossRef] [PubMed]
52. Singh, V. Recent advances and opportunities in synthetic logic gates engineering in living cells. *Syst. Synth. Biol.* **2014**, *8*, 271–282. [CrossRef] [PubMed]